Modulating Artificial Membrane Morphology: pH-Induced Chromatic Transition and Nanostructural Transformation of a Bolaamphiphilic Conjugated Polymer from Blue Helical Ribbons to Red Nanofibers

Jie Song, Quan Cheng,* Susanne Kopta,† and Raymond C. Stevens*

Contribution from the Materials Sciences Division, Lawrence Berkeley National Laboratory, University of California, Berkeley, California 94720

Received September 26, 2000

Abstract: Design and characterization of helical ribbon assemblies of a bolaamphiphilic conjugated polymer and their color-coded transformation into nanofibers are described. An L-glutamic acid modified bolaamphiphilic diacetylene lipid was synthesized and self-assembled into right-handed helical ribbons with micron scale length and nano scale thickness under mild conditions. The ribbon structures were further stabilized by polymerizing well-aligned diacetylene units to form bisfunctional polydiacetylenes (PDAs). Transitions from flat sheets to helical ribbons and tubes were observed by transmission electron microscopy. The helical ribbons appear to originate from the rupture of flat sheets along domain edges and the peeling off between stacked lipid layers. These results point to the applicability of chiral packing theory in bolaamphiphilic supramolecular assemblies. Contact mode atomic force microscopy observations revealed that high order existed in the surface packing arrangement. Hexagonal and pseudorectangular packings were observed in flat and twisted regions of the ribbons, respectively, suggesting a correlation between microscopic morphologies and nanoscopic packing arrangements. The tricarboxylate functionalities of the bolaamphiphilic lipid provide a handle for the manipulation of the bisfunctional PDAs' morphology. Increasing solution pH caused the fraying of helical ribbons into nanofibers accompanied by a sharp blue-to-red chromatic transition. A dramatic change in circular dichroism spectra was observed during this process, suggesting the loss of chirality in packing. A model is proposed to account for the pH-induced morphological change and chromatic transition. The color-coded transition between two distinct microstructures would be useful in the design of sensors and other "smart" nanomaterials requiring defined molecular templates.

Introduction

Since the early 1980s, considerable attention has been drawn toward the fabrication of amphiphilic lipid based self-assembling materials as membrane mimetics for a wide range of applications.[1] Today, these materials are playing important roles in the construction of biosensors,[2] controlled release systems or drug/gene delivery vehicles,[3] synthetic supramolecular immunogens,[4] and many other "smart" nanomachines.[5] Despite the continuing emergence of new applications, however, fundamentals, such as the relationship between the microscopic morphology of the self-assembled systems and the chemical structure and conformation of their constituent lipids, remain to be elucidated. On the practical side, it continues to be challenging to rationally design well-defined functional materials and quickly access highly ordered assemblies under mild conditions.

We are interested in the fabrication of new multifunctional supramolecular assemblies with well-defined physical and chemical properties that can be easily modified for a variety of applications. Classical amphiphilic lipids as membrane mimetics have been extensively studied in this context. Although being used as facile model compounds for many studies, they have limitations in stability, structural and chemical versatility, and ease of self-assembly formation. Bisfunctional lipids complement very well many of the deficiencies of monofunctional lipids and provide improved properties.[6] They tend to form well-defined microstructures under mild conditions and have high biological relevance as mimics of natural transmembrane lipids.[7]

* To whom correspondence should be addressed. Cheng: E-Mail Quan_Cheng@lbl.gov. Phone 1-(510)-486-4125. Fax 1-(510)-486-4995. Stevens: E-mail stevens@scripps.edu. Phone 1-(858)-784-9416. Fax 1-(858)-784-9483.

† Permanent address: Institute of Physics, University of Basel, Basel, Switzerland.

(1) (a) Fendler, J. H. *Biomimetic Membranes*: Wiley: New York, 1982. (b) Fendler, J. H. *Science* **1984**, *223*, 888−894. (c) Ringsdorf, H.; Schlarb, B.; Venzmer, J. *Angew. Chem., Int. Ed. Engl.* **1988**, *27*, 113−158.

(2) (a) Charych, D. H.; Nagy, J. O.; Spevak, W.; Bednarski, M. D. *Science* **1993**, *261*, 585−588. (b) Charych, D.; Cheng, Q.; Reichert, A.; Kuziemko, G.; Stroh, M.; Nagy, J. O.; Spevak, W.; Stevens, R. C. *Chem. Biol.* **1996**, *3*, 113−120. (c) Song, X.; Nolan, J.; Swanson, B. I. *J. Am. Chem. Soc.* **1998**, *120*, 4813−4814 and 11314−11315.

(3) (a) Miller, A. D. *Angew. Chem., Int. Ed. Engl.* **1998**, *37*, 1768−1785. (b) Song, J.; Hollingsworth, R. I. *J. Am. Chem. Soc.* **1999**, *121*, 1851−1861. (c) Bondurant, B.; O'Brien, D. F. *J. Am. Chem. Soc.* **1998**, *120*, 13541−13542.

(4) (a) Reichel, F.; Roelofsen, A. M.; Geurts, H. P. M.; Hamalainen, T. I.; Feiters, M. C.; Boons, G. J. *J. Am. Chem. Soc.* **1999**, *121*, 7989−7997. (b) Reichel, F.; Roelofsen, A. M.; Geurts, H. P. M.; van der Gaast, S. J.; Feiters, M. C.; Boons, G. J. *J. Org. Chem.* **2000**, *65*, 3357−3366.

(5) (a) Fuhrhop, J.-H.; Schnieder, P.; Boekema, E.; Helfrich, W. *J. Am. Chem. Soc.* **1988**, *110*, 2861−2867. (b) Special section, Engineering a Small World. In *Science* **1991**, *254*, 1300−1335. (c) Srisiri, W.; Sisson, T. M.; O'Brien, D. F.; McGrath, K. M.; Han, Y.; Gruner, S. M. *J. Am. Chem. Soc.* **1997**, *119*, 4866−4873. (d) Steinberg-Yfrach, G.; Liddell, P. A.; Hung, S.-C.; Moore, A. L.; Gust, D.; Moore, T. A. *Nature* **1997**, *385*, 239−241.

(6) (a) Bader, H.; Ringsdorf, H. *Faraday Discuss. Chem. Soc.* **1986**, *81*, 329−337. (b) Escamilla, G. H.; Newkome, G. R. *Angew. Chem., Int. Ed. Engl.* **1994**, *33*, 1937−1940. (c) Fyles, T. M.; Loock, D.; Zhou, X. *J. Am. Chem. Soc.* **1998**, *120*, 2997−3003. (d) Meglio, C. D.; Rananavare, S. B.; Svenson, S.; Thompson, D. H. *Langmuir* **2000**, *16*, 128−133.

10.1021/ja0035046 CCC: $20.00
Published on Web 03/15/2001

Scheme 1. Synthesis of L-Glu-Bis-3[a]

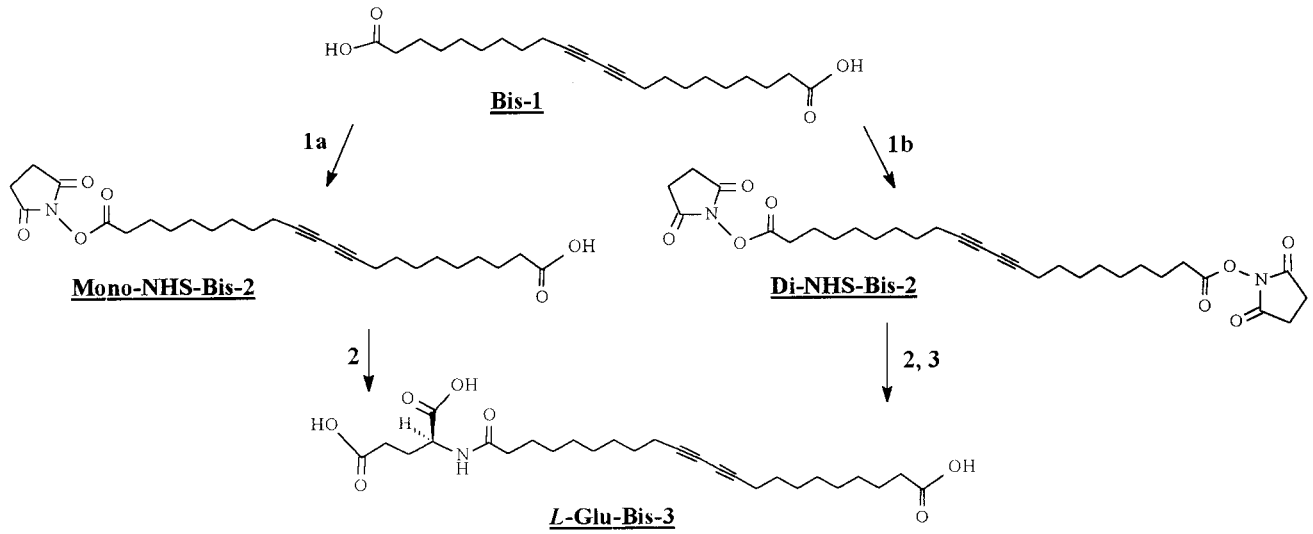

[a] Reagents and conditions: (1a) 1.1 equiv of EDC, 1.1 equiv of NHS, THF−CH_2Cl_2 (5:2 v:v), room-temperature overnight, 61%; (1b) 2.5 equiv of EDC, 2.5 equiv of NHS, THF−CH_2Cl_2 (5:2 v:v), room-temperature overnight, quantitative; (2) 1.1 equiv of L-glutamic acid, Et_3N, THF−H_2O (3:1 v:v), room-temperature, 2 h, 87%; (3) aqueous base, room-temperature, 2 h, quantitative. EDC = 1-(3-dimethylaminopropyl)-3-ethylcarbodiimide hydrochloride; NHS = *N*-hydroxysuccinimide hydrochloride.

The double functionalities of these lipids make them good candidates for the fabrication of materials with asymmetric interfacial properties.

We describe here the design, synthesis, and characterization of an asymmetric bolaamphiphilic lipid **L-Glu-Bis-3** that contains a diacetylene unit at the hydrophobic core, an L-glutamic acid headgroup on one hydrophilic end of the molecule, and a carboxyl group on the other. The tricarboxylate functionalities are expected to bring unique physical and chemical properties to the material and respond to environmental perturbations such as pH elevation in a defined manner. When well-aligned, the diacetylene units can be polymerized and provide a conjugated system with enhanced stability and potentially useful optical properties. Preparation and characterizations of this novel material also afford opportunities to examine the underlying structure−morphology−function relationship of bisfunctional chiral self-assembling systems, on both the microscopic and atomic levels.

Results and Discussions

Design and Synthesis. A robust supramolecular assembly requires strong association between assembling units by different forms of intermolecular forces. The classical amphiphilic lipid assembly can be made more rigid via noncovalent approaches such as increasing van der Waals interaction via $\pi-\pi$ stacking at the lipophilic portion and electrostatic interaction via H-bonding at the hydrophilic portion. The assembly can also be strengthened via covalent modifications such as surface cross-linking, coating, and internal polymerization.[1b,c,5c]

Here, we designed an L-glutamic acid derivatized wedge-shaped bolaamphiphilic diacetylene lipid **L-Glu-Bis-3** (Scheme 1) as the self-assembling unit of a highly organized molecular architecture. Bolaamphiphilic lipids have been shown to readily form well-organized systems under mild conditions.[6] They mimic transmembrane lipids that some microorganisms synthesize for stabilizing membrane structures in response to extreme conditions such as high pH or temperature.[7] Amino acids have been shown to be excellent functional groups for a variety of supramolecular structures, such as vesicles, monolayers, microtubes, ribbons, and sheets.[9,10] They render necessary handedness for building chiral supramolecular assembly and provide handles for further surface modifications and improvement of aggregation properties. In our design, L-glutamic acid was attached to one end of a diacetylene-containing lipid 10,12-docosadiynedioic acid (**Bis-1**) through an amide linkage (Scheme 1). The diacetylene unit was placed at the center of the molecule to maximize the chance of proper alignment of diacetylenes in different packing arrangements. The alignment is critical to the wedge-shaped molecules for the initiation of effective polymerization.[8,11]

The synthesis of **L-Glu-Bis-3** was straightforward. The synthetic route and yields are summarized in Scheme 1. Commercially available diacetylene lipid **Bis-1** was activated on one end with *N*-hydroxysuccinimide[12] before it was coupled with L-glutamic acid through an amide linkage. The selective activation yielded **Mono-NHS-Bis-2** and **Di-NHS-Bis-2** in a 4:1 ratio. **Mono-NHS-Bis-2** was further converted to **L-Glu-Bis-3** with an overall 61% yield. In a modified route, activation of both carboxylate groups before the attachment of glutamic acid and quantitative hydrolysis of the unreacted terminal in the end of the synthesis brought the overall yield up to 87%.

Preparation of the Supramolecular Assembly and Its Polymerization. The self-assembling of matrix lipid **L-Glu-**

(7) (a) Jung, S.; Zeikus, J. G.; Hollingsworth, R. I. *J. Lipid Res.* **1994**, *35*, 1057−1065. (b) Lee, J.; Jung, S.; Lowe, S.; Zeikus, J. G.; Hollingsworth, R. I. *J. Am. Chem. Soc.* **1998**, *120*, 5855−5863.

(8) (a) Frankel, D. A.; O'Brien, D. F. *J. Am. Chem. Soc.* **1991**, *113*, 7436−7437. (b) Frankel, D. A.; O'Brien, D. F. *J. Am. Chem. Soc.* **1994**, *116*, 10057−10069. (c) Thomas, B. T.; Safinya, C. R.; Plano, R. J.; Clark, N. A. *Science* **1995**, *267*, 1635−1638. (d) Kolusheva, S.; Shahal, T.; Jelinek, R. *J. Am. Chem. Soc.* **2000**, *122*, 776−780.

(9) Neumann, R.; Ringdorf, H. *J. Am. Chem. Soc.* **1986**, *108*, 487−490.

(10) (a) Kunitake, T.; Nakashima, N.; Shimomura, M.; Okahata, Y.; Kano, K.; Ogawa, T. *J. Am. Chem. Soc.* **1980**, *102*, 6642−6644. (b) Cescato, C.; Walde, P.; Luisi, P. L. *Langmuir* **1997**, *13*, 4480−4482. (c) Cheng, Q.; Stevens, R. C. *Langmuir* **1998**, *14*, 1974−1976. (d) Cheng, Q.; Yamamoto, M.; Stevens, R. C. *Langmuir* **2000**, *16*, 5333−5342. (e) Cheng, Q.; Fu, J. A.; Burkard, R.; Wang, W.; Yamamoto, M.; Yang, J.; Stevens, R. C. *Thin Solid Films* **1999**, *345*, 292−299.

(11) Okada, S.; Peng, S.; Spevak, W.; Charych, D. *Acc. Chem. Res.* **1998**, *31*, 229−239.

(12) Spevak, W.; Nagy, J. O.; Charych, D. H.; Schaefer, M. E.; Gilbert, J. H.; Bednarski, M. D. *J. Am. Chem. Soc.* **1993**, *115*, 1146−1147.

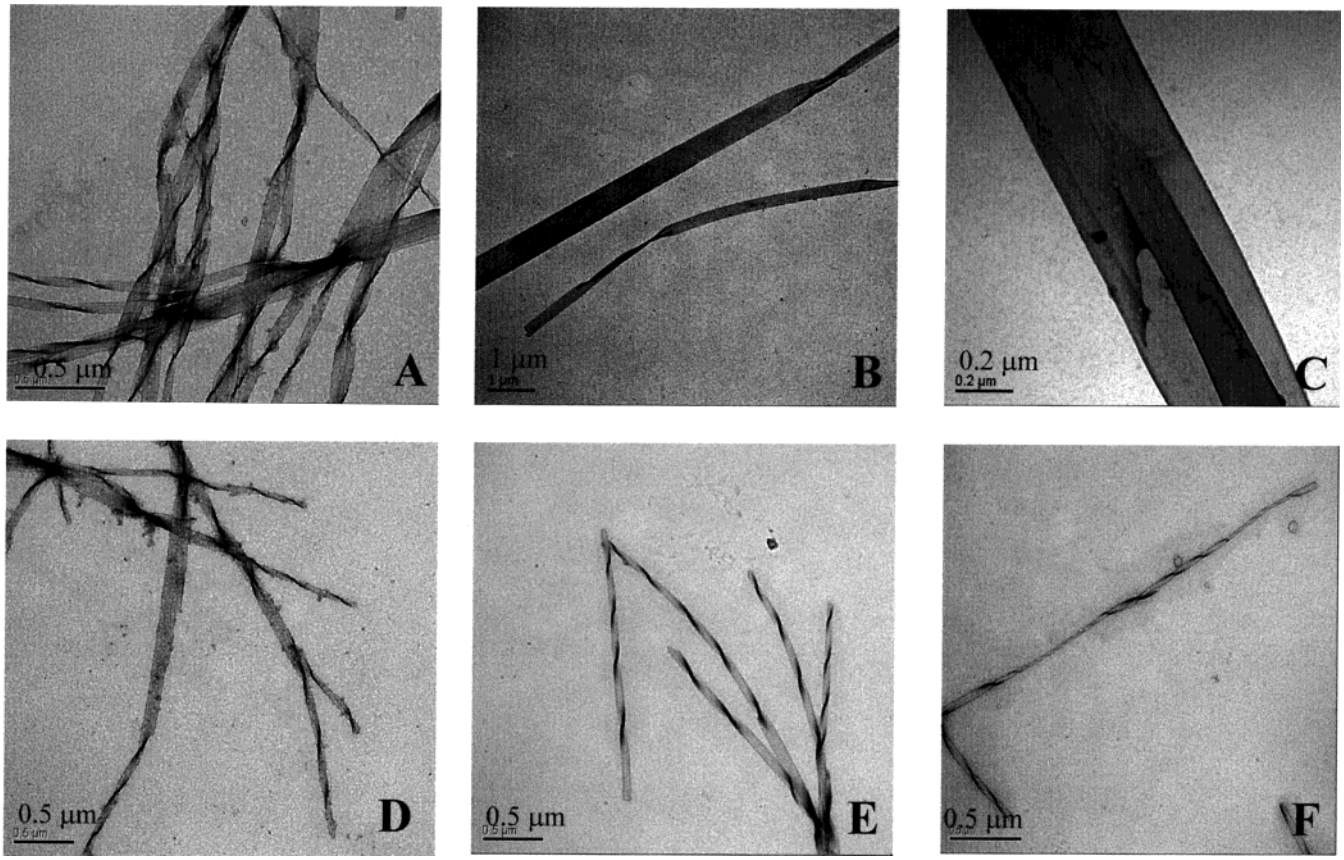

Figure 1. Transmission electron micrographs of **Poly-L-Glu-Bis-3** (0.15 mg/mL). Note the rupture along the domain edges of wide flat ribbons (A) and the origination of helical ribbons from there (A, B, and D). Also note the right-handedness of the helical ribbons (E and F) and the further twisting of ribbons into tubular structure at certain regions (F).

Bis-3 occurred rapidly under mild conditions. Instead of probe sonication and subsequent low-temperature incubation that are commonly used for monofunctional lipids, 2 min of vortexing and 10−20 min of room-temperature incubation was sufficient to ensure the formation of stable supramolecular assembly in aqueous solution for **L-Glu-Bis-3**. UV-irradiation of the assembled material resulted in rapid polymerization of **L-Glu-Bis-3** (within seconds), giving the material a dark blue appearance. The rapid polymerization indicates a highly ordered assembly and the good alignment of diacetylene units. Dynamic light scattering (DSL) indicated that the size of the microstructures was on the scale of microns. Consistent with this, filtration of the polymerized blue assembly through a 1 μm membrane yielded a colorless filtrate that showed no absorption in the visible region.

Solid-state **L-Glu-Bis-3** and **Poly-L-Glu-Bis-3** gave nearly identical FTIR data (spectra shown in the Supporting Information). The spectra were overall poorly resolved due to the material's highly compact packing nature, the existence of multiple chemically nonequivalent carboxylates, H-bonding, and the overlapping of absorption bands (e.g. asymmetric carboxylate $(C{=}O)_2$ stretches overlap with amide I and amide II bands; symmetric $(C{=}O)_2$ stretches overlap with C−N stretch, etc.). The appearance of asymmetric CH_2 stretching at a frequency lower than 2920 cm^{-1} in both forms indicates highly crystalline packing of the oligomethylene chains in the assemblies. As expected, a characteristic intense and broad absorption at 3500−2700 cm^{-1} that corresponds to H-bonded O−H stretch was observed in both forms, indicating H-bonding of carboxylates via either intramolecular or intermolecular mode.

Micro- and Nanoscopic Characterizations: Morphologies and Surface Packing Arrangements. Transmission electron microscopy (TEM) and atomic force microscopy (AFM) were used to characterize the morphology and surface packing arrangement of the material. Transmission electron micrographs confirmed the formation of ribbonlike microstructures with lengths of tens to hundreds of microns in both polymerized and unpolymerized forms. Polymerization of the diacetylenes did not appear to change the morphology of the material. Representative TEM micrographs of the polymeric samples are shown in Figure 1. These assemblies contain microstructures in forms of flat ribbons (Figure 1A−D) and twisted ribbons with various degrees of right-handed helicity (Figure 1E,F). The twisted ribbons adopt a very similar morphology to those formed by bilayer systems containing double chain PDA-phospholipids.[13] Tubular structures were observed as segments of some helical ribbons, apparently resulting from higher regional helicity (Figure 1F). Strips of parallel domains were observed on wider ribbons (Figure 1A−C), with apparently the same direction of the polymer backbone. The thickness of the ribbons was observed between 5 and 10 nm at different regions, suggesting monolayer or double layer packing arrangements, respectively. The widths of the ribbon structures vary from fifty to several hundred nanometers, with generally wider dimensions for flat structures (Figure 1B,C).

To address the morphological stability of the observed microstructures, a kinetics study by TEM was conducted. TEM graphs were obtained for samples incubated at room-temperature for extended hours (up to 18 h) before UV cross-linking was conducted. No significant morphological changes were observed (data not shown), although various degrees of precipitation occurred upon extended incubation. This is different from what was observed in a kinetics study conducted on a double chain

(13) Svenson, S.; Messersmith, P. B. *Langmuir* **1999**, *15*, 4464−4471.

bilayer PDA lipid, where extended incubation at ambient temperature induced a microstructure transformation from nanotubes to helical ribbons.[13] In a different preparation involving probe sonication and subsequent cooling to room-temperature, we obtained the material with similar morphologies: a mixture of flat and helical ribbons. These results seem to suggest that the mild vortex and room-temperature incubation method we described is sufficient for the generation of stable materials with defined morphologies.

Extensive experimental discussions[14,15] and theoretical treatments[16] of the lipid microstructures have been attempted to explain the formation of tubular or helical morphologies. Most theories emphasize the principle of chiral packing. Schnur et al. postulated that when bilayer chiral amphiphilic lipids aggregate, they first form large strips with sharply separated domains.[14] When the original aggregate is larger than the favored ribbon width, such aggregates would then break up along the domain edge to form ribbons that are free to twist into helices by chiral packing effect. Helical ribbons may further fuse into tubular structures to reduce edge energy. Our observations provide evidence to support this theory in the case of the chiral bolaamphiphilic lipid system. TEM micrographs of **L-Glu-Bis-3** and **Poly-L-Glu-Bis-3** captured the apparent initiation of the transition from flat strips to helical ribbons through rupturing of wider flat strips along the domain edges (Figure 1A) or peeling off between two stacked layers (Figure 1D). With optimal width and thickness, the smaller strips could then twist into helical structures as a result of these chiral molecules' cumulative tilt away from the local surface normal. Formation of tubular structures, as observed at certain regions, is evidence of further winding of the helical ribbons upon the initial twisting process (Figure 1F).

There have been debates on the role of molecular chirality in the formation of tubular and helical microstructures.[16] Our system is slightly more complex when compared to bilayer chiral lipids. For the bolaamphiphilic lipid studied here, the chiral glutamic acid residue was attached to one end of the molecule, giving an overall wedge-shaped geometry. There are two possible packing arrangements: (1) glutamic acid groups alternately pack with the smaller carboxyl groups, thereby generating two comparable layer surfaces, or (2) the large glutamic acid residues pack on the same side of the layer surface, generating a biased chiral face with increased curvature. As discussed earlier, two major forms of microstructures, flat ribbons and helical structures, were observed. The alternating arrangement of headgroups may be favorable for the close packing of diacetylene units because it induces less steric hindrance and electrostatic repulsion between large glutamic headgroups. This could be the predominant format of organizations when the system first self-assembles into relatively wide flat ribbons. Driven by chiral packing and the further relief of unfavorable headgroup interactions, each assembling lipid would then start to tilt away from its nearest neighbor and lead to the formation of helical structures. Alternatively, the highly biased headgroup arrangement that results in large surface curvatures may also promote the formation of highly twisted helical ribbons.

To understand the relationship between the microscopic morphology and molecular arrangements, detailed study on the packing of lipids in the assembly at a much smaller scale must be performed. Atomic force microscopy (AFM) has proven useful for the direct investigation of surface structure and long-range order of monofunctional polydiacetylene lipids[17a,b] and some bolaamphiphilic systems with identical headgroups.[17c,d] We used contact mode AFM to characterize the molecular packing of lipid microstructures on atomic level. Figure 2A shows microscopic images of a typical flat ribbon and a twisted ribbon with dimensions consistent with those observed in transmission electron micrographs shown in Figure 1 (panels B and C). High-resolution scans over a relatively flat helical ribbon surface revealed a highly organized two-dimensional hexagonal packing arrangement at the nanoscopic scale (Figure 2B). The bright spots on the AFM image represent arrays of terminal carboxylate groups. There are two carboxylates on the glutamate-terminated end of the lipid. One packing scenario is that only the outer terminal carboxylate on the glutamate end is exposed to the surface so that each bright spot on AFM only corresponds to one bolaamphiphilic molecule. In this case, the conventional interpretation of AFM data for alkyl-terminated lipids is applicable. Another possibility is that both carboxylates are exposed to the surface and therefore each glutamate would lead to two bright spots on the surface array. In this case, the assignment of unit cell and the calculation of area per molecule can be complicated. We believe that the second packing scenario is an unlikely case due to the following reasons: (1) Facing both carboxylates toward the surface would unfavorably expose the hydrophobic alkyl portion of the glutamate toward the aqueous environment and (2) isotherms of the Langmuir monolayer of analogous glutamate-terminated bilayer diacetylene lipid revealed a limiting molecular area comparable to that for the single carboxylate-terminated diacetylene lipid,[10e] which clearly excludes the packing arrangement where both carboxylates on the glutamate end are exposed to the surface in the crystalline state. Based on one carboxylate per lipid surface exposure, the AFM data analysis can be performed in a conventional way. It is worth pointing out, however, trying to distinguish the terminal carboxylate on the glutamate end from the one on the single carboxylate end, thereby distinguishing biased packing from alternating packing based on this AFM data would be very difficult. The 2-D fast Fourier Transformation (2-D FFT) suggests an approximate cell area of 20 Å^2 ($a = b = 4.8 \pm 0.2$ Å; $\gamma = 60 \pm 3°$), which is characteristic for tightly packed hydrocarbon chains.[18] Charych et al. reported the study on thermochromic monofunctional PDA films using AFM. Their results showed that the highly ordered hexagonal packing arrangement was not obtained at room-temperature for the blue phase film even when it was overcompressed during the preparation.[17a] Instead, the pseudorectangular packing arrangement was predominantly observed. Our results here demonstrate that **L-Glu-Bis-3** is able to form more stable, more

(14) (a) Schnur, J. M. *Science* **1993**, *262*, 1669−1676. (b) Schnur, J. M.; Ratna, B. R.; Selinger, J. V.; Singh, A.; Jyothi, G.; Easwaran, K. R. K. *Science* **1994**, *264*, 945−947.

(15) (a) Fuhrhop, J.-H.; Schnieder, P.; Rosenberg, J.; Boekema, E. *J. Am. Chem. Soc.* **1987**, *109*, 3387−3390. (b) Chung, D. S.; Benedek, G. B.; Konikoff, F. M.; Donovan, J. M. *Proc. Natl. Acad. Sci. U.S.A.* **1993**, *90*, 11341. (c) Chappell, J. S.; Yager, P. *Chem. Phys. Lipids* **1991**, *58*, 253.

(16) (a) Selinger, J. V.; MacKintosh, F. C.; Schnur, J. M. *Phys. Rev. E* **1996**, *53*, 3804−3818. (b) Thomas, B. N.; Lindemann, C. M.; Clark, N. A. *Phys. Rev. E* **1999**, *59*, 3040−3047. (c) de Gennes, P.-G. *C. R. Acad. Sci. Paris* **1987**, *304*, 259. (d) Lubensky, T. C.; Prost, J. *J. Phys. (France) II* **1992**, *2*, 371. (e) Helfrich, W.; Prost, J. *Phys. Rev. A* **1988**, *38*, 3065. (f) Ou-Yang, Z.-C.; Liu, J.-X. *Phys. Rev. Lett.* **1991**, *43*, 6826. (g) Nelson, P.; Powers, T. *Phys. Rev. Lett.* **1992**, *69*, 3409.

(17) (a) Lio, A.; Reichert, A.; Ahn, D. J.; Nagy, J. O.; Salmeron, M.; Charych, D. H. *Langmuir* **1997**, *13*, 6524−6532. (b) Thomas, B. N.; Corcoran, R. C.; Cotant, C. L.; Lindemann, C. M.; Kirsch, J. E.; Persichini, P. J. *J. Am. Chem. Soc.* **1998**, *120*, 12178−12186. (c) Kogiso, M.; Ohnishi, S.; Yase, K.; Masuda, M.; Shimizu, T. *Langmuir* **1998**, *14*, 4978−4986. (d) Shimizu, T.; Ohnishi, S.; Kogiso, M. *Angew. Chem., Int. Ed.* **1998**, *37*, 7, 3260−3262.

(18) Kuzmenko, I.; Kaganer, V. M.; Leiserowitz, L. *Langmuir* **1998**, *14*, 3882−3888.

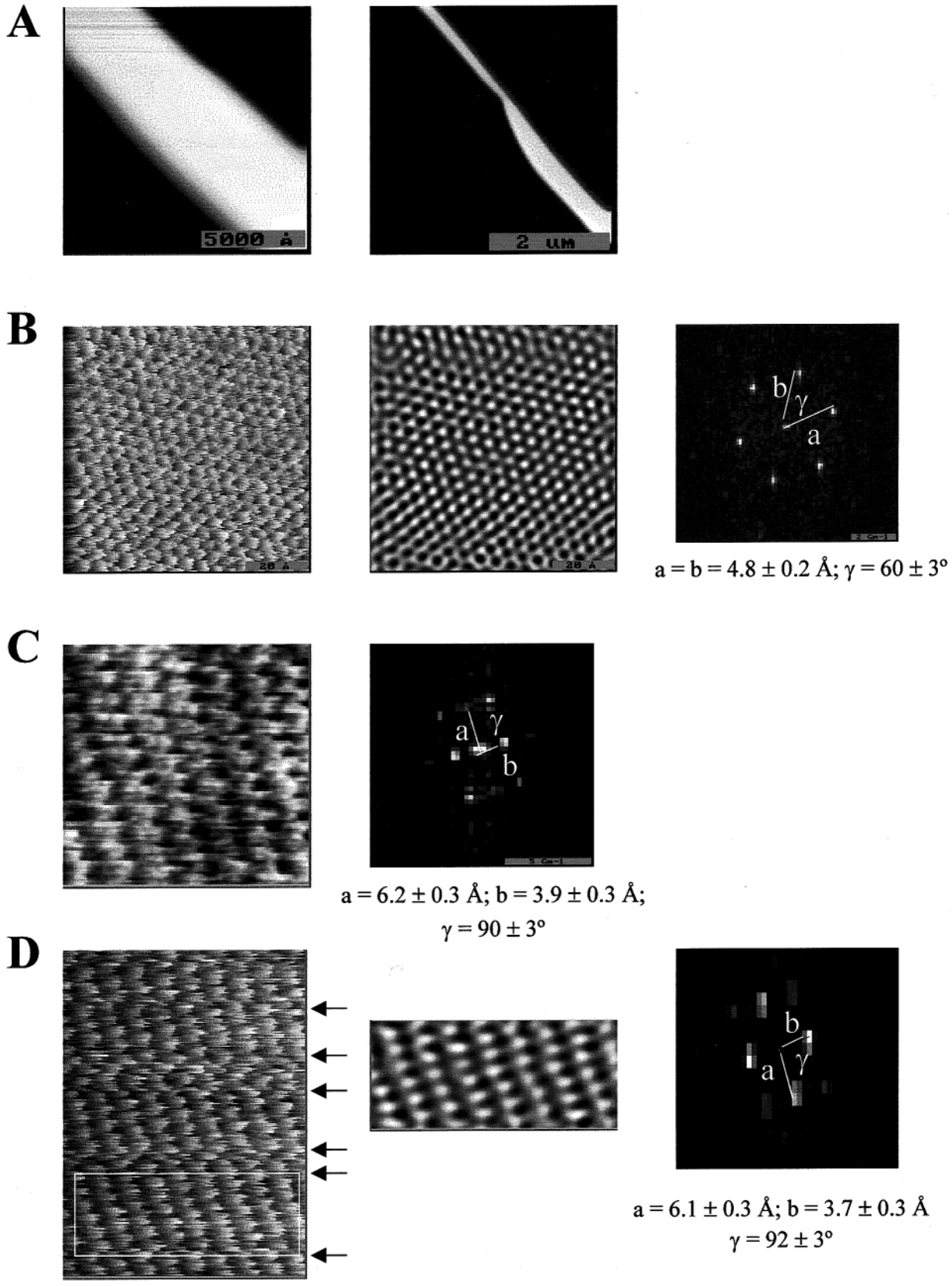

Figure 2. Contact mode atomic force microscopy (AFM) images of **Poly-L-Glu-Bis-3**. (A) A flat ribbon (left; image size 1 μm × 1 μm) and a twisted ribbon (right; image size 4 μm × 4 μm). (B) High-resolution frictional force image obtained on a flat ribbon: raw data, filtered data (image size 80 Å × 80 Å), 2-D FFT spectrum of the high resolution image and the corresponding hexagonal unit cell dimensions. (C) High-resolution frictional force image obtained on a highly twisted area of a helical ribbon (image size 45.5 Å × 45.0 Å), its 2-D FFT spectrum, and the corresponding unit cell dimensions. (D) Left: High-resolution frictional force images obtained on a highly twisted area of a helical ribbon (image size 59.7 Å × 80.4 Å). Arrows denote lateral dislocations. Center: Filtered image of the boxed area (image size 50.6 Å × 22.3 Å). Right: 2-D FFT of the zoom-in area and the corresponding unit cell dimensions.

compact, and better-organized assemblies at ambient conditions, and is therefore suitable for the fabrication of highly ordered functional organic supramolecular assemblies under mild conditions.

Scans of a twisted ribbon area showed a different atomic surface packing arrangement (Figure 2C,D). 2-D FFT of a typical high-resolution image (Figure 2C) revealed a pseudorectangular unit cell with a cell area of approximately 24 Å^2 ($a = 6.2 \pm 0.3$ Å; $b = 3.9 \pm 0.3$ Å; $\gamma = 90 \pm 3°$). Two possible scenarios or the combination of them could account for the increase in unit cell area. First, the increase in unit cell area may be a result of the increased molecular tilt away from the local surface normal at the helical region. Second, relatively loose packing is expected in the highly curved region. The system has to be less rigid in areas of curvature and a less closely packed cell such as a highly distorted hexagonal or pseudorectangular cell would be more favorable than a hexagonal one. It is worth noting that when the scanning tip swept through the top of the three-dimensional ribbon structure, regional fluctuations would occur and sometimes led to lateral dislocations in the frictional force images as indicated by the arrows in Figure 2D. However, similar images were observed over several consecutive scans. The pseudorectangular packing arrangement was still observed in the 2D-FFT (Figure 2D, right) of the boxed area in Figure 2D (left). Repeated scans did not cause any damage to either form of the microstructures, suggesting the system's robust organization.

The AFM study of the bisfunctional PDA lipid microstructures demonstrates the difference in packing arrangement between helical ribbon structures and thin films formed by the monofunctional PDA lipid. Moreover, our results reveal that there is a shift in molecular packing and an increase in unit cell dimension when the microstructure undergoes a morphological twist. Morphological changes such as vesicle-to-tubule transformations in diacetylene lipid systems have been elegantly studied with X-ray diffraction technique and calorimetry.[8c,19] Here our AFM study provides an alternative approach to explore this area. The results suggest a strong correlation between packing arrangements at the atomic scale and morphologies of the material at the micron scale, as characterized by hexagonal and pseudorectangular packing arrangements at flat and highly twisted regions of the microstructure, respectively.

pH-Induced Chromatic Transition and Morphological Transformation. Tricarboxylate functionalities in the PDA matrix lipid are expected to have strong impact on the material's optical properties and packing arrangement, particularly in the event of pH change, as observed previously by our group.[10c,d]

Colorimetric properties of the bisfunctional conjugated polymer were studied. As expected, electrostatic repulsion between headgroups caused by pH elevation led to the typical blue-to-red transition of the conjugated polydiacetylene (PDA) polymer. Although new insights continue to be provided for further understanding of chromatic transitions of PDAs,[20] it has been generally accepted that environmental perturbations, such as mechanical stress[21] (mechanochromism), high temperature[22] (thermochromism), surface binding events[2] (biochromism), or extreme pH conditions that cause electrostatic repulsion between the PDA lipids,[10c,d] would induce strains and distortions within the pendant side chains and the conjugated ene−yne backbone.[23] Such influence would result in a shortened conjugation network and absorption of light at a shorter wavelength. Figure 5A shows the colorimetric response (CR) of **Poly-L-Glu-Bis-3** as a function of pH. A sharp blue-to-red color change was observed upon the increase of pH. Because of the existence of multiple carboxylate groups in the molecule, the chromatic transition occurred at a more acidic pH region compared to the glutamic acid derivatized bilayer polydiacetylene lipids.[10c,d] At pH 7.5, the **Poly-L-Glu-Bis-3** blue polymer turned completely red. The UV−vis absorbance spectra of both red and blue forms of the polymer are shown in Figure 5B.

TEM images of base-treated **Poly-L-Glu-Bis-3** (Figure 3) showed dramatic changes in the morphology of microstructures. All helical ribbons and flat sheets were frayed into thin nanofibers upon the increase of pH. It appears that the weakly associated network of fibers with defined direction were formed first (Figure 3A,B) before they were completely torn apart to form randomly coiled fibers (Figure 3C,D). By increasing pH from 7.5 to 9 or prolonging the exposure time to these basic conditions, we were able to observe more randomly coiled fibers. The diameters of these fibers were estimated below 10 nm.

From the conditions used to trigger the morphological change, it is apparent that the transformation was caused by increased electrostatic repulsion developed between the deprotonated carboxylate headgroups at higher pH. Higher surface negative charges split closely packed polymer chains and resulted in thin fibers with less than 10 nm in diameter. Figure 4 illustrates a tentative model of the scenario. The front view of the split polymer resembles a tubular micellar block copolymer with stacked conjugated polymer backbones as a rigid core and saturated lipid side chains as floppy arms capped with charged hydrophilic headgroups. Indeed, the pH split nanofibers observed here bear very close resemblance to some carefully designed rod−coil copolymers in terms of microscopic morphology.[24] The pH-induced splitting of ribbons to thin nanofibers suggests that linear propagation is the predominant format of polymerization of diacetylene units in this system.

AFM characterization of the molecular packing of the nanofibers was attempted. Unfortunately, high fidelity images could not be obtained. These fibers were easily brushed away by the scanning tip due to lack of strong adhesion of the material to the substrate.

An earlier study on monofunctional PDA lipid morphology with AFM[17a] showed 10−20 nm wide parallel stripelike features within a single PDA domain. Not enough evidence is available to allow a conclusion to be drawn on the smallest dimension of the cluster of PDA polymer chains. Our observation on the formation of 10 nm wide fibers from the splitting along domain edges of wider bisfunctional PDA ribbons in response to pH elevation is consistent with the data from this earlier study. This suggested that the smallest width of optimal subdomains of such PDA aggregations, especially in aqueous solution, could be around or below 10 nm.

In addition to UV−vis and TEM, we employed other spectroscopic methods, particularly Circular Dichroism (CD) spectroscopy, to characterize the pH induced chromatic transition

(19) (a) Caffery, M.; Hogan, J.; Rudolph, A. S. *Biochemistry* **1991**, *30*, 2134−2146. (b) Burke, T. G.; Rudolph, A. S.; Price, R. R.; Sheridan, J. P.; Dalziel, A. W.; Singh, A.; Schoen, P. E. *Chem. Phys. Lipids* **1988**, *48*, 215−230.

(20) (a) Foley, J. L.; Li, L.; Sandman, D. J.; Vela, M. J.; Foxman, B. M.; Albro, R.; Eckhardt, C. J. *J. Am. Chem. Soc.* **1999**, *121*, 7262−7263. (b) Huo, Q.; Russell, K. C.; Leblanc, R. M. *Langmuir* **1999**, *15*, 3972−3980.

(21) Galiotis, C.; Yong, R. J.; Batchelder, D. N. *J. Polym. Sci. Polym. Phys. Ed.* **1983**, *21*, 2483.

(22) Wenzel, M.; Atkinson, G. H. *J. Am. Chem. Soc*. **1989**, *111*, 6123.

(23) Eckhardt, H.; Boudreaux, D. S.; Chance, R. R. *J. Chem. Phys*. **1986**, *85*, 4116.

(24) Wang, H.; Wang, H. H.; Urban, V. S.; Littrell, K. C.; Thiyagarajan, P.; Yu, L. *J. Am. Chem. Soc*. **2000**, *122*, 6855−6861.

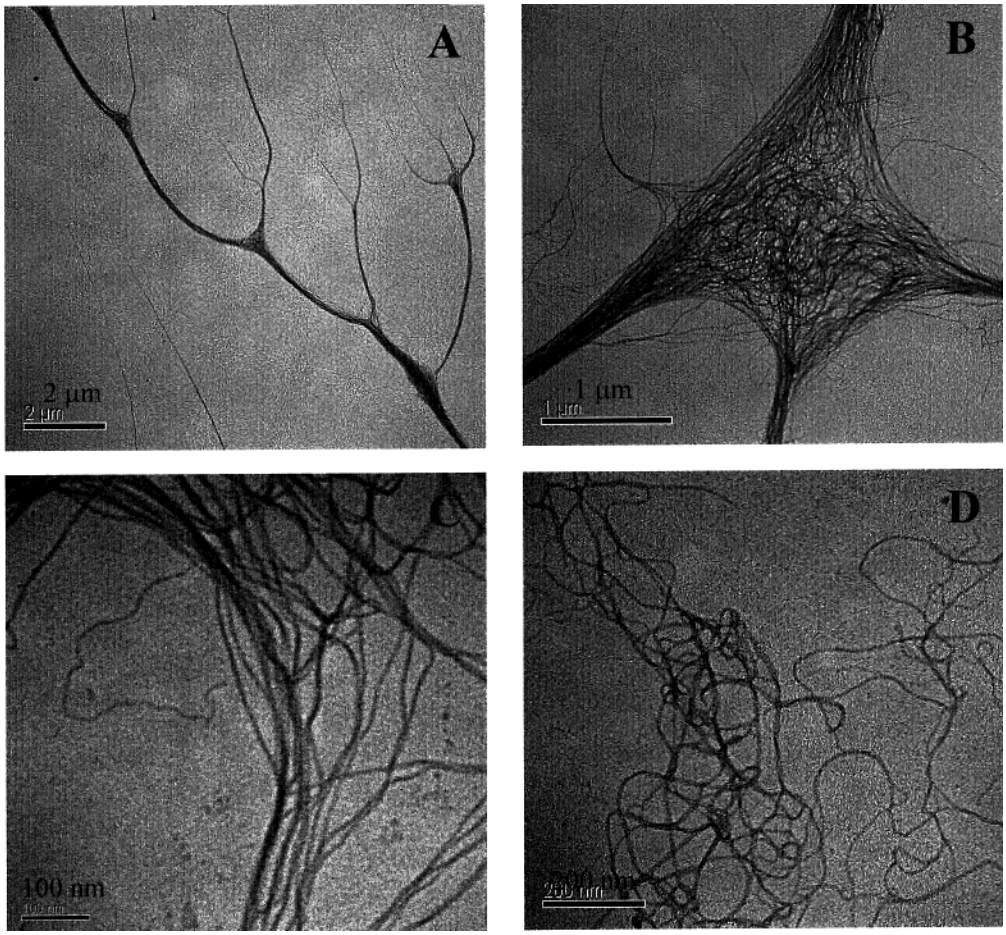

Figure 3. Transmission electron micrographs of base-treated **Poly-L-Glu-Bis-3** (A, B, and C: treated with pH 7.5 Tris buffer; D: treated with pH 9 Tris buffer). Note the coexistence of networks of nanofibers with defined directions (A and B) and randomly coiled fibers (C and D).

and morphological transformations. CD spectra can provide empirical evidence of protein and nucleic acid secondary structures. They are also useful in studying chiralities of synthetic self-assembling aggregates where chirality originates from the chiral packing of assembling molecules.[25] A dramatic change in molar ellipticity θ was observed when the **Poly-L-Glu-Bis-3** assembly was transformed from right-handed helical ribbons to frayed fibers by pH increase (Figure 6). The intense absorption band of **Poly-L-Glu-Bis-3** around 200 nm agreed with literature data where the self-assembling of bilayer amphiphilic PDA lipids yielded helical ribbon and tubular structures.[25] The comparison between CD spectra of **Poly-L-Glu-Bis-3** before (curve A) and after (curve B) the base treatment showed dramatic loss in molar ellipticity (almost 90%) accompanying the morphological transformation of the assembly, clearly indicating the massive loss of chiral microstructures (helical ribbons and tubes) during the transformation. The new microstructures (nanofibers) formed under basic conditions only passed on an insufficient amount, if any, of the chiral packing arrangement to contribute to the overall chirality in the assembly.

Conclusions

In conclusion, we have designed and synthesized a novel chiral bisfunctional transmembrane diacetylene lipid that rapidly self-assembles into robust right-handed helical ribbon structures under mild conditions. The assemblies are also readily cross-linked to form blue conjugated polymers with retained morphology. By taking advantage of the pH sensitivity of the chiral amino acid headgroup of the bolaamphiphile, we were able to trigger a morphological transformation of the polymer from blue helical ribbons to red nanofibers, which was further accompanied by a loss of handedness in the packing arrangement. The alignment of the conjugated nanofibers could be controlled through experimental optimization. The color-coded transition between two distinct microstructures opens possibilities in applications where defined molecular templates are the basis for a variety of sensing or triggering mechanisms.

TEM, AFM, and CD characterizations of the lipid microstructures provided direct and detailed evidence supporting chiral packing theory in the assembly formed by transmembrane lipid **L-Glu-Bis-3**. AFM data suggest that flat ribbons and highly twisted ribbons correlate with hexagonal and pseudorectangular packing arrangements on the atomic level, respectively. The study offers insight into the relationship between the material's microscopic morphology and molecular packing arrangement. Future studies will focus on revealing molecular packings in red-phase PDA nanofibers and the fine-tuning of the morphological transition.

Experimental Section

Materials. 10,12-Docosadiynedioic acid (**Bis-1**) was obtained in 95% purity from Lancaster, and was further purified by dissolving it in tetrahydrofuran (THF) and passing it through a short silica pad prior to use to remove blue polymerized impurities. Anhydrous THF used in the lipid activation step was purchased from Aldrich. Water used in the preparation of various buffer solutions was purified with the

(25) (a) Spector, M. S.; Easwaran, K. R. K.; Jyothi, G.; Selinger, J. V.; Singh, A.; Schnur, J. M. *Proc. Natl. Acad. Sci. U.S.A.* **1996**, *93*, 12943−12946. (b) Spector, M. S.; Selinger, J. V.; Singh, A.; Rodriguez, J. M.; Price, R. R.; Schnur, J. M. *Langmuir* **1998**, *14*, 3493−3500.

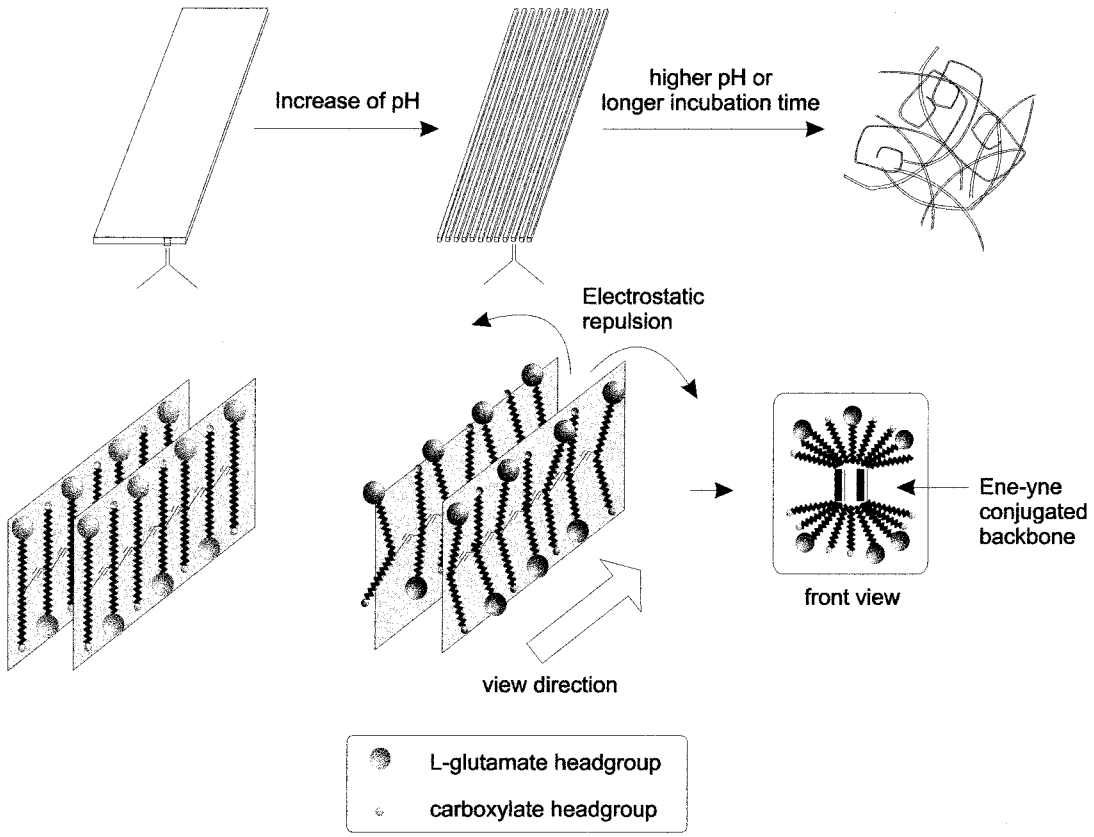

Figure 4. Proposed model of pH-triggered morphological transformation of **Poly-L-Glu-Bis-3** from helical ribbons to nanofibers. Note: The polar headgroup arrangement in this cartoon does not reflect the actual molecular packing details.

Millipore Milli-Q system. Other chemicals were reagent grade and used without further purification.

Synthesis. (a) General Techniques. Flash column chromatography was performed on Aldrich silica gel (60 Å, 230−400 mesh). Yields refer to chromatographically and spectroscopically (^{1}H NMR) homogeneous materials. NMR spectra were recorded on a Bruker DRX-500 spectrometer. Chemical shifts are reported relative to the solvent peak. In the case where mixed solvents of methanol, chloroform, and water were used, methanol was chosen as the reference. The high-resolution mass spectrum (HRMS) was recorded on a VG ZAB spectrometer with Fast Atom Bombardment (FAB) conditions and an *N*-benzyl alcohol (NBA) matrix at the positive mode.

(b) Mono-NHS-Bis-2. To a solution of **Bis-1** (1.2 g, 3.3 mmol) in THF (50 mL) was added 1-(3-dimethylaminopropyl)-3-ethylcarbodiimide hydrochloride (EDC, 0.7 g, 3.6 mmol) in dichloromethane (20 mL) followed by *N*-hydroxysuccinimide hydrochloride (NHS, 0.42 g, 3.6 mmol). The mixture was stirred at room-temperature overnight followed by the removal of solvent by rotary evaporation. The residue was extracted with chloroform and saturated brine. The organic layer was dried with anhydrous sodium sulfate and concentrated. Pure **Mono-NHS-Bis-2** (0.93 g, 61%) was obtained by flash column chromatography. **Di-NHS-Bis-2** (0.29 g, 16%) was also isolated along with the recovery of unconverted **Bis-1**. ^{1}H NMR ($CDCl_3$ with trace CD_3OD, 500 MHz): δ 2.79 (4H, b), 2.55 (2H, t, $J = 7$ Hz), 2.23 (2H, t, $J = 7$ Hz), 2.18 (4H, t, $J = 7.5$ Hz), 1.68 (2H, m), 1.55 (2H, m), 1.45 (4H, m), 1.32 (m), 1.26 (m). ^{13}C NMR ($CDCl_3$ with trace CD_3OD, 125 MHz): δ 176.15, 169.42, 168.41, 76.86, 64.93, 33.60, 30.38, 29.77, 28.65, 28.62, 28.44, 28.29, 28.22, 28.20, 27.87, 27.84, 25.14, 24.43, 24.08, 18.62.

(c) Di-NHS-Bis-2. Using the above procedure with an excess amount of EDC (2.5 equiv) and NHS (2.5 equiv), **Di-NHS-Bis-2** was obtained in multigram scale in >95% yield. ^{1}H NMR ($CDCl_3$, 500 MHz): δ 2.84 (8H, b), 2.57 (4H, t, $J = 7.5$ Hz), 2.22 (4H, t, $J = 7$ Hz), 1.71 (4H, t, $J = 7.5$ Hz), 1.49 (8H, t, $J = 7.5$ Hz), 1.37 (m), 1.29 (m). ^{13}C NMR ($CDCl_3$, 125 MHz): δ 169.18, 168.63, 77.45, 65.25, 30.88, 28.84, 28.73, 28.64, 28.22, 25.56, 24.50, 19.13.

(d) L-Glu-Bis-3. Triethylamine was added dropwise to a suspension of L-glutamic acid (80 mg, 0.54 mmol) in water (5 mL) until a homogeneous solution was obtained (pH 8−9). This solution was then slowly introduced to a solution of **Mono-NHS-Bis-2** (220 mg, 0.48 mmol) in THF (15 mL). The mixture was stirred for 2 h prior to the addition of 3 mL of water and the adjustment of pH to 3 by 1 N hydrochloric acid. THF was removed by rotary evaporation and the remaining aqueous mixture was extracted with ethyl acetate. The organic layer was dried over anhydrous sodium sulfate, filtered, and then concentrated by rotary evaporation. The product was purified by flash column chromatography (1:1 chloroform/methanol with 1% v/v water, R_f 0.45) and 204 mg (87%) of **L-Glu-Bis-3** was obtained. Similar yield was obtained reacting 0.55 equiv of **Di-NHS-Bis-2** with 1 equiv of L-glutamic acid, followed by hydrolysis in aqueous basic solution. ^{1}H NMR ($CDCl_3$ and CD_3OD with trace D_2O, 500 MHz): δ 4.15 (1H, m), 2.20 (m), 1.99 (1H, m), 1.86 (1H, m), 1.55 (4H, m), 1.47 (4H, m), 1.34 (m), 1.27 (m). ^{13}C NMR ($CDCl_3$ and CD_3OD with trace D_2O, 125 MHz): δ 176.70, 174.39, 77.15, 77.11, 64.88, 64.85, 48.99, 35.87, 33.83, 28.87, 28.81, 28.71, 28.68, 28.58, 28.49, 28.40, 28.32, 27.92, 27.87, 25.31, 24.53, 18.66. HRMS FAB$^+$ (NBA): $C_{27}O_7NH_{41}Na$ [M + Na]$^+$, calcd 514.2781, found 514.2769.

Supramolecular Aggregates Preparation. Two milliliters of 0.1 N sodium chloride aqueous solution was added to 0.3 mg of **L-Glu-Bis-3**. The mixture was vortexed for 2 min and a clear, colorless solution was obtained. The aggregate was incubated 20 min at ambient temperature before UV irradiation or other measurements were taken. For the kinetics study on microstructure formation, the aggregates were incubated for extended time (1, 2, 5, and 18 h) at ambient temperature before UV irradiation was performed. As a control experiment, probe sonication of the lipid suspension was performed for 20 min with a 40W probe sonicator. The resulting clear solution was allowed to cool to room-temperature before another 20 min incubation at the same temperature was allowed.

Cross-linking of the Supramolecular Aggregates. Freshly prepared supramolecular aggregates were loaded onto 96-well polystyrene tissue culture plates and irradiated with UV light (254 nm, CL 1000 Ultraviolet

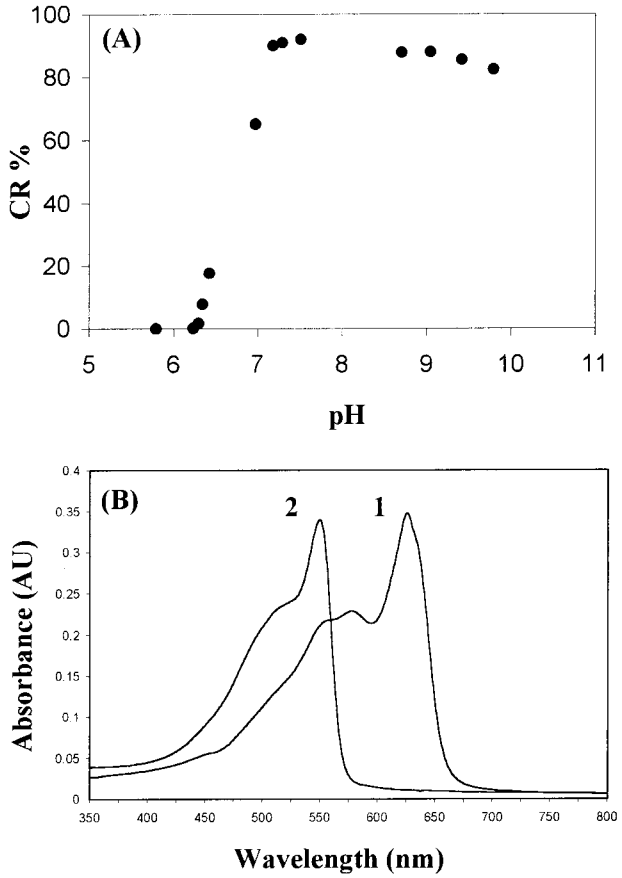

Figure 5. (A) Colorimetric response (CR) of **Poly-L-Glu-Bis-3** to pH elevation. (B) Absorbance of blue (curve 1) and red forms (curve 2, adjusted by pH 7.5 Tris buffer) of **Poly-L-Glu-Bis-3.**

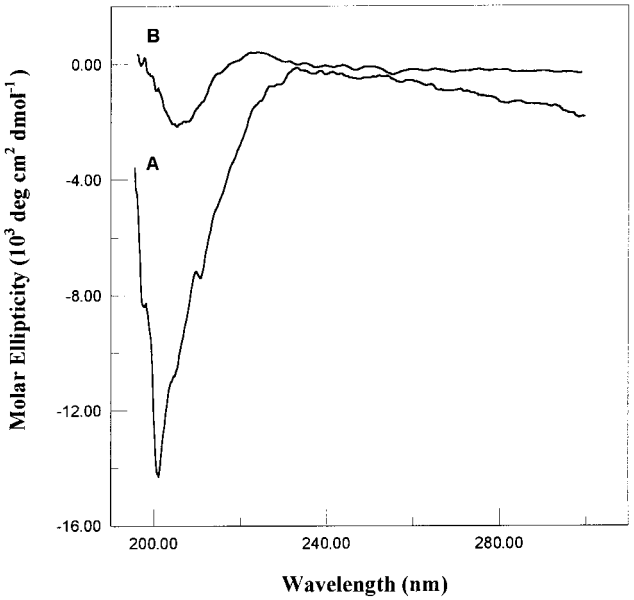

Figure 6. CD spectra of **Poly-L-Glu-Bis-3**: (A) 0.15 mg/mL (0.1 N aqueous NaCl) and (B) with the addition of 10% (v/v) pH 9 Tris buffer (25 mM Tris, 0.1 N aqueous NaCl).

Crosslinker). Cross-linking occurred rapidly and uniform dark blue color developed in less than 12 s of exposure time. However, longer irradiation (1−2 min) was applied to ensure the formation of extended conjugation networks.

UV−Visible and FTIR Spectroscopy. Visible absorption spectra were recorded on a Shimadzu UV-1601 spectrometer at ambient temperature. Poly-L-Glu-Bis-3 (0.3 mg/mL, 0.1 N aqueous NaCl) was diluted 10-fold (with 0.1 N aqueous NaCl) before the absorption spectrum was taken. The sample was then passed through a 1 μm membrane (Whatman 4 mm syringe filter, polysulfone filter with polypropylene housing). The colorless filtrate was collected and its absorption spectrum recorded as above. FTIR spectra were obtained on a Perkin-Elmer System 2000 FTIR spectrometer. Solid sample was well ground with dry KBr powder and compressed into a transparent disk.

Dynamic Light Scattering (DSL) Experiments. Size distributions of the supramolecular aggregates were determined on a Coulter N4 Plus particle analyzer with a 90° detector angle. A 200 nm latex bead standard was used for calibration.

Measurements of Colorimetric Response (CR) as a Function of pH. Freshly cross-linked **Poly-L-Glu-Bis-3** solution was loaded on a 96-well transparent tissue culture plate (100 μL per well). Two microliters of a sodium hydroxide solution (with a gradient of [OH^-] from 6 to 10^{-4} M) was added to each well. The resulting solutions were then allowed to stand at ambient temperature for 30 min to stabilize the blue-to-red color change. The pH values of the resulting solutions were measured by a Corning Semi-micro pH Electrode (epoxy body). The colorimetric response (CR) to the pH increase was then recorded on a SPECTRAmax 250 Microplate Spectrophotometer supported by SOFTmax PRO Microplate Analysis software (Molecular Devices Corporation). CR was measured as the percent change in the absorption at 630 nm (blue form polydiacetylene) relative to the total absorption at 630 and 550 nm (red form polydiacetylene). The initial percentage of the blue phase is defined as $B_0 = I_{630}/(I_{630} + I_{550})$. The same value was calculated for the pH elevated solution (B_{pH}). CR is therefore defined as the percentage change in blue form (B) upon the addition of base: $CR = [(B_0 - B_{pH})/B_0] \times 100\%$.

Transmission Electron Microscopy (TEM). TEM images of the supramolecular aggregates were obtained on both polymerized and unpolymerized forms with a Zeiss electron microscope operating at 80 kV. Samples were freshly made and deposited on carbon film coated Cu grids. Though the microstructures of diacetylene lipids are readily visualizable owing to the high electron density, negative staining with 0.5% uranyl acetate was performed to enhance the image quality.

Atomic Force Microscopy (AFM). Ten microliters of cross-linked **L-Glu-Bis-3** (0.15 mg/mL, in 0.1 N aqueous NaCl) was spin-coated on a freshly cleaved Muscovite mica substrate. AFM was obtained on a home-built instrument[26] controlled by a commercial electronics unit (RHK technology, Troy, MI). The AFM was enclosed in a box with ambient conditions of 21 °C and approximately 50% relative humidity. One silicon cantilever (Park Scientific Instruments) with a nominal force constant of 0.4 N/m and a measured tip radius of 150 nm was used.

Circular Dichroism (CD) Spectroscopy. CD measurements were performed on both the cross-linked **Poly-L-Glu-Bis-3** (0.15 mg/mL, in 0.1 N aqueous NaCl) and the pH elevated polymer sample. For the latter, 10% volume of pH 9 Tris buffer (25 mM Tris, 0.1 N aqueous NaCl) was added to the **Poly-L-Glu-Bis-3** (0.15 mg/mL, in 0.1 N aqueous NaCl). The original homogeneous blue solution turned red instantly upon the addition of the buffer. CD spectra were recorded on a JASCO J-600 spectropolarimeter.

Acknowledgment. This work is supported by the Director, Office of Nonproliferation and National Security, Office of Research and Development of the U.S. Department of Energy under Contract No. DE-AC03-76SF00098. The authors thank Dr. Peter R. David and Prof. Rawle I. Hollingsworth for critical reading of the manuscript, Dr. Ivan Kuzmenko for many helpful discussions, and Dr. Mark Alper, Program Director of the Center for Advanced Materials, Biomolecular Materials Program, for continued encouragement and support of this research program.

Supporting Information Available: FTIR spectra of **L-Glu-Bis-3** and **poly-L-Glu-Bis-3** (PDF). This material is available free of charge via the Internet at http://pubs.acs.org.

JA0035046

(26) Kolbe, W. F.; Ogletree, D. F.; Salmeron, M. B. *Ultramicroscopy* **1992**, *42−44*, 1113−1117.